Taylor & Francis
Taylor & Francis Group

ORIGINAL RESEARCH

OPEN ACCESS | Check for updates

Galectin-3 inhibition with belapectin combined with anti-OX40 therapy reprograms the tumor microenvironment to favor anti-tumor immunity

Elizabeth R. Sturgill[a], Annah S. Rolig [a], Stefanie N. Linch[a], Courtney Mick[a], Melissa J. Kasiewicz[a], Zhaoyu Sun[a], Peter G. Traber[b], Harold Shlevin[c], and William L. Redmond [a]

aEarle A. Chiles Research Institute, Providence Cancer Institute, Portland, OR, USA; bUniversity of Pennsylvania School of Medicine, Philadelphia, PA, USA; cGalectin Therapeutics, , Norcross, GA, USA

ABSTRACT

Treatment with an agonist anti-OX40 antibody (aOX40) boosts anti-tumor immunity by providing costimulation and driving effector T cell responses. However, tumor-induced immune suppression contributes significantly to poor response rates to aOX40 therapy, thus combining aOX40 with other agents that relieve tumor-mediated immune suppression may significantly improve outcomes. Once such target is galectin-3 (Gal-3), which drives tumor-induced immunosuppression by increasing macrophage infiltration and M2 polarization, restricting TCR signaling, and inducing T cell apoptosis. A wide-variety of tumors also upregulate Gal-3, which is associated with poor prognosis. Tumor-bearing (MCA-205 sarcoma, 4T1 mammary carcinoma, TRAMP-C1 prostate adenocarcinoma) mice were treated with a Gal-3 inhibitor (belapectin; GR-MD-02), aOX40, or combination therapy and the extent of tumor growth was determined. The phenotype and function of tumor-infiltrating lymphocytes was determined by flow cytometry, multiplex cytokine assay, and multiplex immunohistochemistry. Gal-3 inhibition synergized with aOX40 to promote tumor regression and increase survival. Specifically, aOX40/belapectin therapy significantly improved survival of tumor-bearing mice through a CD8+ T cell-dependent mechanism. Combination aOX40/belapectin therapy enhanced CD8+ T cell density within the tumor and reduced the frequency and proliferation of regulatory Foxp3+CD4+ T cells. Further, aOX40/belapectin therapy significantly reduced monocytic MDSC (M-MDSCs) and MHC-IIhi macrophage populations, both of which displayed reduced arginase 1 and increased iNOS. Combination aOX40/belapectin therapy alleviated M-MDSC-specific functional suppression compared to M-MDSCs isolated from untreated tumors. Our data suggests that Gal-3 inhibition plus aOX40 therapy reduces M-MDSC-mediated immune suppression thereby increasing CD8+ T cell recruitment leading to increased tumor regression and survival.

Background

Cancer immunotherapy is now considered the "fifth pillar" of cancer therapy alongside surgery, radiation, chemotherapy, and targeted therapy[1]. One of the most effective types of cancer immunotherapy is immune checkpoint blockade with anti-PD-1 or anti-CTLA-4 monoclonal antibodies (mAb), which alleviate immune suppression. Another immunotherapy approach is boosting anti-tumor immunity by providing T cell costimulation with agonist mAbs directed against members of the Tumor Necrosis Factor Receptor (TNFR) family, such as OX40 (CD134), 4–1BB (CD137), and CD27. For example, in pre-clinical and clinical studies, agonist anti-OX40 mAb (aOX40) treatment augments effector T cell responses capable of supporting anti-tumor immunity.[2–5] Despite the success of cancer immunotherapy,[6] one issue limiting response rates is tumor-induced immunosuppression. How to overcome this immunosuppression in order to unleash more potent anti-tumor immunity is a central, unresolved issue in cancer immunotherapy. Here, we test the hypothesis that inhibition of the immunosuppressive molecule galectin-3 (Gal-3), will synergize with agonist aOX40 therapy to promote tumor regression, increase response rates to immunotherapy, and improve overall survival.

T cell costimulation with OX40-specific agonists induces robust T cell activation and anti-tumor immunity. Specifically, aOX40 therapy promotes a differentiated T cell effector state characterized by increased cytolytic function (IFN-γ, granzyme B), cytokine release (IL-2), and survival.[3–5,7–9] Further, aOX40 treatment can reverse anergy in tumor-reactive CD8+ T cells.[2,10,11] Altogether, as demonstrated by pre-clinical work, aOX40-induced CD8+ T cell activity facilitates tumor regression. The first-in-human phase I clinical trial with an agonist anti-human OX40 mAb (NCT01644968), similarly led to increased proliferation of CD4+ and CD8+ T cells, and 12 of 30 patients (40%) experienced regression of at least one metastatic lesion. Importantly, only mild to moderate side effects were reported.[12] Currently, research on improving the response to aOX40 therapy is focused on combining OX40 agonists with other therapeutic modalities that alleviate immune suppression, such as checkpoint inhibition (e.g. aOX40/aCTLA-4).[10,13,14]

One mediator of tumor-induced immunosuppression that can be targeted pharmacologically is Gal-3,[15–18] a molecule that is upregulated in a wide variety of tumors and is associated with both poor prognosis and reduced response to immunotherapy.[19–22] In fact, tumors that are low or deficient in Gal-3 are more likely to respond to checkpoint blockade,[21] thus making Gal-3 blockade an attractive target for combination with T cell-targeting immunotherapies. Gal-3 is a lectin family member with a C-terminal carbohydrate-binding domain that recognizes distinct N-glycan moieties found on glycoproteins. In addition to this carbohydrate-binding domain, Gal-3 has a non-lectin N-terminal domain, which is unique to Gal-3 among the galectin family and allows Gal-3 to oligomerize into pentamers. Gal-3 pentamers can bind multiple glycans, forming complexes that crosslink a number of glycosylated ligands to form a dynamic lattice structure.[15,16,23] The Gal-3 lattice structures can dysregulate T cell activation, thus promoting immunosuppression. For example, a Gal-3 lattice binds multiple T-cell receptor (TCR) glycoproteins, restricting their mobility and ability to cluster, thus reducing antigen sensitivity and T cell activation.[16,24] Further, Gal-3 can bind glycosylated cytokines, which hinders cytokine diffusion within the tumor microenvironment (TME) and can result in reduced CD8$^+$ T cell recruitment to the tumor.[25] Finally, Gal-3 can polarize macrophages toward an M2 (pro-tumor) phenotype via sustained activation of PI3K downstream of CD98 binding,[26] and preliminary evidence suggests that Gal-3 recruits myeloid cells to the tumor site, thereby increasing myeloid-derived suppressor cells (MDSC) within tumors.[27,28]

Herein, we tested the hypothesis that Gal-3 inhibition plus aOX40 therapy would synergize to promote tumor regression and increase survival via a reduction in tumor-induced immune suppression. We tested this hypothesis using a novel Gal-3 inhibitor, belapectin, which is generated from naturally occurring carbohydrate polymers. Belapectin prevents Gal-3 from binding glycans and thus prevents lattice formation and subsequent immunosuppression.[29] belapectin appears safe and well tolerated and is therefore well positioned for use in combination with immunotherapies.[30] Our data demonstrates that Gal-3 inhibition in conjunction with aOX40 therapy significantly reduced tumor progression compared to either therapy alone. This efficacy occurred through a reduction in MDSC infiltration and suppression and a concomitant increase in T cell effector function. Overall, these data indicate that belapectin plus aOX40 is a novel immunotherapy combination capable of reducing tumor-induced immunosuppression to augment anti-tumor immunity in preclinical models.

Methods

Mice and cell lines

Wild-type C57BL/6 and BALB/c mice were purchased from Jackson Labs (Bar Harbor, ME). Experimental procedures were performed following the National Institutes of Health Guide for the Care and Use of Laboratory Animals and under the supervision of the Institutional Animal Care and Use Committee at Providence Cancer Institute. MCA-205 (sarcoma), TRAMP-C1 (prostate adenocarcinoma), and 4T1 (mammary carcinoma) cells were grown to confluence in RPMI 1640 (Lonza, Walkersville, MD) supplemented with 10% fetal bovine serum (FBS), 1 M HEPES, 100 mM sodium pyruvate, non-essential amino acids, and penicillin/streptomycin/glutamine (ThermoFisher).

In vitro experiments

For Gal-3 expression/secretion, 1.5×10^5 cells of each tumor line were seeded into a 24-well flat bottom plate. After 24 hours, supernatants were removed, centrifuged, and used in a Gal-3 ELISA, as per manufacturer's instructions (Ray Biotech). To monitor cell growth and apoptosis, each tumor cell line was seeded at 5×10^3 cells per well of a 96-well plate. After 24 hours, cells were treated with either 0.2 mg/ml (light blue) or 2 mg/ml (purple) belapectin, then monitored for 48 hours for confluence and apoptosis using Incucyte Caspase-3/7 green dye (Sartorius), following manufacturer's instructions. Cells were monitored for 60-hours post-treatment.

In vivo tumor growth and antibody/inhibitor treatment

1.5×10^6 MCA-205 (flank), 1.0×10^6 TRAMP-C1 (flank), or 5×10^4 4T1 (mammary fat pad) tumor cells were implanted subcutaneously into wild-type mice. Tumor growth (area) was assessed every 2–3 days with micro-calipers and mice were sacrificed when tumors exceeded 150 mm^2. Tumor-bearing mice were treated (ip) with rat IgG (250 μg; Sigma Aldrich) or anti-OX40 mAb (250 μg; clone OX86) (days 4, 8) with and without belapectin (2.4 mg/dose; 3x/week for 2 weeks). For tumor harvest, tumor-bearing mice were treated with IgG or anti-OX40 (days 10, 14) with or without belapectin (days 10, 12, 14, 16). Tumor-infiltrating lymphocytes (TIL) were harvested by cutting tumors into small fragments followed by digestion in 1 mg/ml collagenase and 20 mg/ml DNase (Sigma Aldrich) in RPMI 1640 for 45 min at room temperature. TIL were filtered through 70 μm nylon mesh, then stained for analysis by flow cytometry. For CD8$^+$ T cell depletion studies, anti-CD8 antibody (10 mg/kg; 2x/week; clone 53–6.7; Bio-X-Cell) was administered. For CD4$^+$ T cell depletion studies, anti-CD4 antibody (10 mg/kg; 1x/week; clone GK1.5; Bio-X-Cell) was administered, tumor area was measured every 2–3 days as indicated above.

Lymphocyte isolation and analysis

Peripheral lymph nodes and spleens were harvested and processed to obtain single-cell suspensions. ACK lysing buffer (Lonza) was added for 2 min at RT to lyse red blood cells. Cells were then rinsed with complete RPMI (cRPMI) 1640 medium supplemented with 10% FBS, 1 M HEPES, 100 mM sodium pyruvate, non-essential amino acids, and penicillin/streptomycin/glutamine (ThermoFisher). To obtain peripheral blood lymphocytes, peripheral blood was collected from mice via the submandibular vein into tubes containing 50 μl heparin. Cells were resuspended in 1 ml of flow cytometry buffer (0.5% FBS, 0.02% NaN$_3$ in PBS) and 700 μl of lymphocyte separation media (Lonza) was underlain prior to centrifugation. Lymphocytes were collected from the interface, washed, and analyzed by flow cytometry. To measure cytokine production, lymphocytes were incubated in 96-well plates previously

coated with aCD3/aCD28 mAbs (2 and 5 μg/ml, respectfully) in 10% cRPMI and 1.0 μl/ml GolgiPlug solution (BD Biosciences) for 4 h at 37°C. After washing, cells were stained and analyzed by flow cytometry.

Flow cytometry

Cells were stained for 30 min at 4°C with: FoxP3 (MF23) PE-CF594, Ki-67 (B56) FITC, Ly6G (1A8) FITC (BD Biosciences, San Jose, CA), CD4 (RM4-5) BV650, CD8 (53–6.7) BV785, CD11b (M1/70) BV785, CD11c (M418) FITC, CD19 (6D5) FITC, CD45 (30-F11) BV421, CD45 (30-F11) BV570, CD206 (C068C2) PE, F4/80 (BM8) BV510, IL-10 (JES5-16E3) APC, IL-4 (11B11) BV421, Lag-3 (C9B7W) PerCP-Cy5.5, LAG-3 (C9B7W) APC, Ly6C (HK1.4) BV510, Ly6C (HK1.4) PerCP-Cy5.5, NKp46 (29A1.4) APC, PD-1 (29 F.1A12) PE-Cy7, PD-L1 (10 F.92 G) BV711 (BioLegend, San Diego, CA), CD8 (53–6.7) APC, CD11b (M1/70) FITC, CD11b (M1/70) PE, CD45 (30-F11) APC, Fixable Viability Dye eFluor 780, Granzyme A (GzA-3G8.5) APC, IFN-γ (XMG1.2) PE, MHC-II (M5/144.15.2) FITC, TNF-α (TN3-19) PE-Cy7 (ThermoFisher), CD3 (17A2) APC, CD19 (6D5) APC, FoxP3 (FJK16a) eF450, iNOS (CXNFT) PE-Cy7, MHC-II (M5/114.15.2) eF450, NKp46 (29A1.4) FITC (ThermoFisher), Arg1 (Cat: IC5868A) APC, and TIM-3 (215008) PE (R&D, Minneapolis, MN). For intracellular stains, cells were fixed and permeabilized using the FoxP3 Staining Buffer kit (ThermoFisher). For experiments that required the sorting of CD11b$^+$Ly6C$^+$, CD4$^+$, or CD8$^+$ T cells, TILs were filtered through 70 μm nylon mesh followed by a CD45$^+$ positive selection using a CD45 (TIL) Microbeads kit (Miltenyi Biotec) and an autoMACS Pro Separator (Miltenyi Biotec). Where indicated, cells were sorted on a FACSAria II Cell Sorter (BD Biosciences) into 1.7 ml tubes containing 400 μl cRPMI. To analyze the suppression assay, CFSE MFI was measured on a Fortessa SORP (BD Biosciences) or LSRII flow cytometer. All analysis was done with FACSDiva (BD Biosciences) and FlowJo software (BD Biosciences).

Cytokine bead array

Supernatant was collected from sorted CD4$^+$ and CD8$^+$ T-cells cultured in the presence of aCD3/aCD28 (2 and 5 μg/ml, respectively) coated 24-well plate for 24 hours for a CBA using a ProcartaPlex Mouse Cytokine/Chemokine Panel 1A 36-Plex kit (EPX360-26012-901; Invitrogen). Data was acquired on a Luminex 200 (R&D Systems).

Suppression assay

CD11b$^+$Ly6C$^+$ cells were sorted from tumors by flow cytometry and then cocultured with 5×10^4 CFSE-labeled naïve CD8$^+$ T cells isolated from the spleens of wild-type mice (Dynabeads Untouched Mouse CD8 T Cells Negative Isolation Kit; ThermoFisher) plus 2×10^5 accessory cells (CD3$^-$ splenocytes) in a 96-well round bottom plate coated with aCD3/aCD28 (2 and 5 μg/mL, respectively). Cells were incubated at 37°C for

72 hours and then the extent of CFSE dilution was determined by flow cytometry.

CFSE labeling

Purified CD8$^+$ T-cells were resuspended at $5-10 \times 10^6$ cells/mL in 0.1% BSA (Fisher Bioreagents) and labeled with 1 μl CFSE (C34554; Invitrogen), immediately followed by vortexing to ensure even CFSE labeling on all cells. The suspension was incubated at 37°C for 10 min, then 10x the volume of cold cRPMI was added. Cells were resuspended at a concentration of 1.0×10^6 cells/mL in 10% cRPMI prior to coculturing with MDSCs.

Multiplex immunohistochemistry

Tumor tissue sections (5 μm) were cut from zinc-fixed, paraffin-embedded blocks. These sections were left to dry overnight in the oven at 37°C on saline-coated Superfrost Plus microscope slides (Fisher Scientific) or until completely dry. Anti-iNOS and anti-Arg1 mAbs were optimized using murine iNOS$^{-/-}$ or Arg1$^{-/-}$ brain or liver tissue as negative controls, respectively. iNOS$^{-/-}$ tissue specimens were kindly provided by Dr. Carol Colton (Duke) and Arg1$^{-/-}$ tissue by Dr. Gerry Lipshutz (UCLA). Single-plex chromogenic and TSA-Opal immunofluorescence stains were performed on serial sections for optimizing each biomarker in the panel. Before performing mIHC, the sections were deparaffinized in xylene, rehydrated through gradient ethanols, and diH$_2$O. Tissue sections were rinsed in 1X TBS before heat-induced epitope retrieval (HIER) using Rodent Decloaker (BioCare Medical) in the microwave oven for 15 min. Rodent Decloaker was refilled every 5 min. Sections were washed with diH$_2$O and 1 X TBS, then the sections were circled with PAP pen before incubation with 3% H$_2$O$_2$. After the sections were blocked with antibody diluent/block (PerkinElmer), the first biomarker anti-F4/80 (1:1000, BM8, eBioscience) was stained. The second biomarker anti-iNOS (1:400, rabbit polyclonal, Abcam) was stained after antibody stripping was performed using citrate buffer pH 6.0 in the microwave oven. Tris-EDTA pH9.0 was used for stripping antibodies and further retrieving the epitopes at the same time. Then the following biomarkers were stained: anti-Arg1 (1:64,000, Rabbit Polyclonal, Genetex), anti-CD8 (1:400, 4SM15; eBioscience), anti-CD11b (1:20,000, EPR1344; Abcam), and anti-CD3 (1:100, SP7, SpringBio). Antibody stripping was performed using citrate buffer pH6.0 in the microwave oven before staining the next biomarker except CD8. 3% H$_2$O$_2$ at RT was used instead for this biomarker. MACH2 Rb HRP-Polymer (RHRP520H), MACH2 M HRP-Polymer (MHRP520H), or rat anti-mouse HRP-Polymer was chosen as a secondary antibody in terms of the species of the primary antibody. Opal 620 (1:200), Opal 650 (1:400), Opal 690 (1:400), Opal 570 (1:200), Opal540 (1:400), and Opal520 (1:200) (all from PerkinElmer) were used for detection. Counterstaining was done with DAPI (1 drop of DAPI solution into 0.5 ml of TBST, PerkinElmer) for 5 min at RT. After a quick wash with 1X TBST, the slides were mounted with Prolong Diamond Antifade Mountant (p36970, ThermoFisher). Slides were scanned with a Vectra

Automated Quantitative Pathology Imaging System and images were acquired with Inform Advanced Image Analysis Software (Akoya Biosciences).

Clonogenic analysis of 4T1 metastasis

For clonogenic analysis of spontaneous metastasis in 4T1 tumor-bearing mice, lungs were dissected into 2 mm fragments followed by agitation in 1 mg/mL collagenase (Invitrogen), 100 μg/mL hyaluronidase (Sigma, St Louis, MO), and 20 mg/mL DNase (Sigma) in 1X PBS for 1 hr at RT. Lung digests were filtered through 100 μm nylon mesh and then serial dilutions of cells were seeded into 6-well tissue culture plates in media containing 60 μM 6-thioguanine to select for cancer cells over stromal cells and colonies were counted after 7 days.[31] The serial dilution and the colony count were used to calculate the number of clonogenic cancer cells in the original organ.[32]

Statistical analysis

Statistical significance was determined by unpaired Student t-test (for comparison between two groups), one-way ANOVA for (comparison among three or more groups), or Kaplan-Meier survival (for tumor survival studies) using GraphPad Prism software (GraphPad, San Diego, CA); a p-value of <0.05 was considered significant.

Results

Combined aOX40/belapectin therapy improves survival and reduces metastases

For these experiments we selected 4T1 (mammary carcinoma), TRAMP-C1 (prostate adenocarcinoma), and MCA-205 (sarcoma) tumors, of which TRAMP-C1 and MCA-205 express Gal-3 on the surface and all lines secrete Gal-3 at various levels (Fig. S1). Initially, we tested whether treatment with the Gal-3 inhibitor belapectin *in vitro* affected tumor cell proliferation or apoptosis. There was some decrease in proliferation and a minimal increase in apoptosis of 4T1 and MCA-205 cells in the presence of belapectin, but no impact was observed on TRAMP-C1 cell (Fig. S2). To test the effects *in vivo*, we implanted 4T1, TRAMP-C1, or MCA-205 tumors into wild-type mice followed by treatment with control Ab (rat IgG), aOX40, belapectin, or aOX40/belapectin (Figure 1a). All mice had palpable tumors (>4 mm²) at the start of treatment. Following treatment, we observed a significant reduction in tumor growth and corresponding increase in survival only in response to combined aOX40/belapectin treatment compared to monotherapies across all three tumor types (Figure 1(b-e), Fig. S4), suggesting any direct action of belapectin on tumor cells observed *in vitro* (Fig. S2) did not translate to an *in vivo* effect. We confirmed that combination therapy generated durable long-term memory as 100% tumor-free mice were protected from subsequent tumor re-challenge. Belapectin also enhanced the efficacy of checkpoint blockade (aPD-L1) immunotherapy (Fig. S4). Next, we asked whether adaptive immune responses were responsible for the efficacy of combination therapy by depleting either CD4⁺ or CD8⁺ T cells from mice prior to the initiation of aOX40/belapectin therapy. CD8⁺ T cell depletion completely abrogated the effects of aOX40/belapectin therapy, as survival was reduced to that of IgG controls (figure 1f), while CD4⁺ T cell depletion did not alter survival rates from those observed in immune-competent mice (figure 1f).

Because Gal-3 influences cancer cell adherence, migration, and metastases,[22,23,33] in addition to its direct influence on anti-tumor immune responses, we asked whether aOX40/belapectin therapy reduced the incidence of spontaneous lung metastases that develop in 4T1 tumor-bearing mice. We observed a marked reduction in lung metastases following aOX40/belapectin therapy, including an increased percentage of mice with no detectable lung metastases (22%) compared to those treated with monotherapies alone (Figure 1g). Together, these data suggest aOX40/belapectin therapy significantly improve anti-tumor immunity in a CD8⁺ T cell-dependent manner, while also reducing tumor cell metastases, leading to increased tumor-free survival.

Combination aOX40/belapectin therapy increases CD8⁺ T cell density in the tumor

Given that the therapeutic efficacy of aOX40/belapectin was CD8⁺ T cell-dependent (figure 1f), we examined the phenotype of tumor-infiltrating lymphocytes (TIL) in MCA-205 tumor-bearing mice. We found no significant changes in the percent of CD8⁺, CD4⁺ T effector (Foxp3⁻, Teff), or CD4⁺ T regulatory (Foxp3⁺, Treg) cells across treatment groups (Figure 2a), although there was an upward trend in CD8⁺ and CD4⁺ Teff and a concomitant downward trend in Tregs following aOX40 treatment, similar to previous observations.[3] Similarly, proliferating (Ki-67⁺) and granzyme-producing CD8⁺ T cells trended up after aOX40 treatment but did not reach significance (Figure 2a). However, both CD4⁺ Teff and Treg in the tumor had significantly decreased proliferation (Ki-67) following aOX40/belapectin therapy (Figure 2a). We assessed the functional potential of the TILs by examining cytokine production. While there was no change in Th2 cytokine secretion (IL-4, IL-5, IL-6, IL-13) across treatment groups, there was a trend toward increased Th1 cytokine secretion (IL-2, TNF-α) after combination therapy compared to controls (Fig. S5A). There was also significantly increased IFN-γ secretion in the CD8⁺ T cell compartment, which was primarily driven by aOX40 therapy (Fig. S5B).

While the frequency of CD8⁺ T cells within the tumor was not changed significantly across treatment groups (Figure 2a), the density (# cells/mm² tumor) of CD8⁺ T cells within the tumor was significantly increased following combination therapy as compared to controls, confirmed by flow cytometry (Figure 2b) and multiplex immunohistochemistry (mIHC) (Fig. S6). Similarly, CD4⁺ Teff and Treg cells were present at a higher density after treatment with aOX40 (Figure 2b, middle and right panels, respectively). We also asked whether combination therapy changed the ratio of effector CD8⁺ or CD4⁺ T cells to CD4⁺ Treg, but found no significant differences in these ratios, though there was a trend toward increased ratios in the combination therapy cohort (Figure 2c).
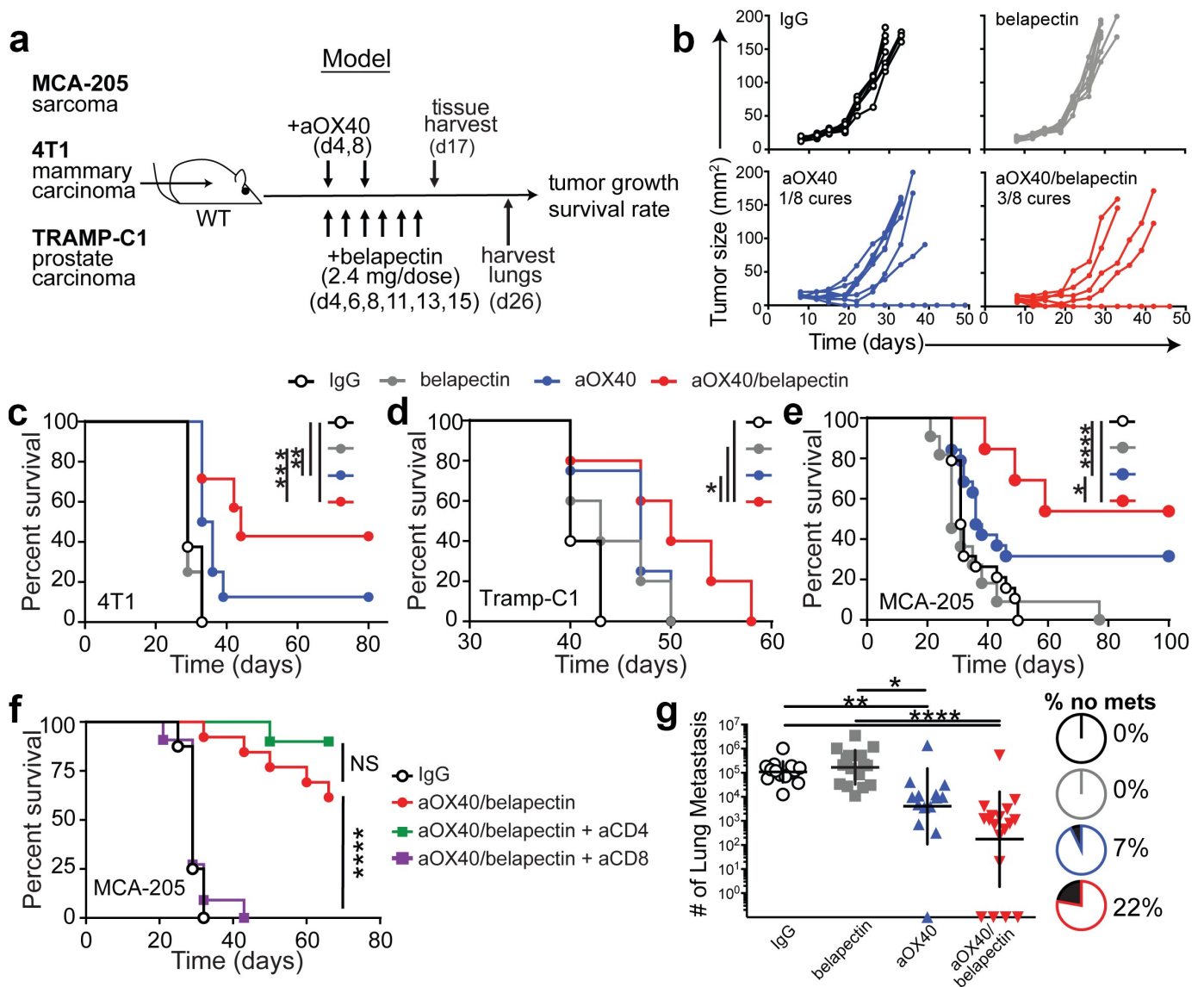
Figure 1. Combined aOX40/belapectin therapy improves survival and reduces metastases. A) Schematic of experimental protocol. 4T1 mammary carcinoma cells were implanted orthotopically (mammary fat pad) in female BALB/c mice, while MCA-205 (sarcoma) or TRAMP-C1 (prostate) tumor cells were implanted subcutaneously in female or male C57BL/6 mice, respectively. Mice were treated with IgG or aOX40 (days 4, 8) with and without belapectin (days 4, 6, 8, 11, 13, 15). B) 4T1 tumor growth was determined across the four treatment groups. C-E) Survival of mice implanted with C) 4T1, D) TRAMP-C1, or E) MCA-205 tumors that were monitored biweekly and euthanized when tumor area reached >150 mm^2 (n = 7–14/cohort). *P < .05, **P < .01, ***P < .001; ***P < .0001; Log-Rank test. F) Survival of MCA-205 tumor-bearing mice treated with aOX40/belapectin therapy (as in A) along with CD4$^+$ or CD8$^+$ T cell depletion. G) Spontaneous lung metastases from 4T1 tumor-bearing mice were determined by clonogenic assay. Graph depicts data from n = 3 independent experiments, *P < .05, **P < .01, ****P < .0001; 1-way ANOVA.

Because aOX40/belapectin combination therapy increased CD8$^+$ T cell density within the tumor (Figure 2b), we asked whether combination therapy affected T cell priming in the lymph node (LN). Within the LN, the frequency of CD8$^+$ T cells and CD4$^+$ Teff cells remained the same across all treatments (Figure 2d); however, we did observe an increased frequency of CD4$^+$ Treg cells (Figure 2d), which was driven primarily by aOX40 immunotherapy. CD8$^+$ T cells, CD4$^+$ Teff, and CD4$^+$ Treg populations all exhibited significantly increased proliferation (Ki-67), also due primarily to OX40-mediated co-stimulation (Figure 2d). As expected, aOX40 therapy increased granzyme B expression in CD8$^+$ T cells and this increase was not enhanced by belapectin (Figure 2d). However, aOX40/belapectin therapy significantly increased CD8$^+$ T cell proliferation in the LN over vehicle and belapectin-only

controls (Figure 2d), which may reflect increased priming in the LN and may provide some rationale for the increased CD8$^+$ T cell density found in the tumor.

aOX40/belapectin therapy decreases M-MDSCs in the tumor

To understand further the mechanism driving increased survival following aOX40/belapectin treatment, we examined other cell types likely to be influenced by Gal-3 inhibition, primarily myeloid cells and MDSCs. Myeloid cells within the TME are a heterogeneous population of cells that includes monocytic MDSCs (M-MDSC; CD11b$^+$Ly6C^{hi}Ly6G^{lo}), polymorphonuclear MDSCs (PMN-MDSC; CD11b$^+$Ly6C^{int}Ly6G^{hi}), and tumor-associated
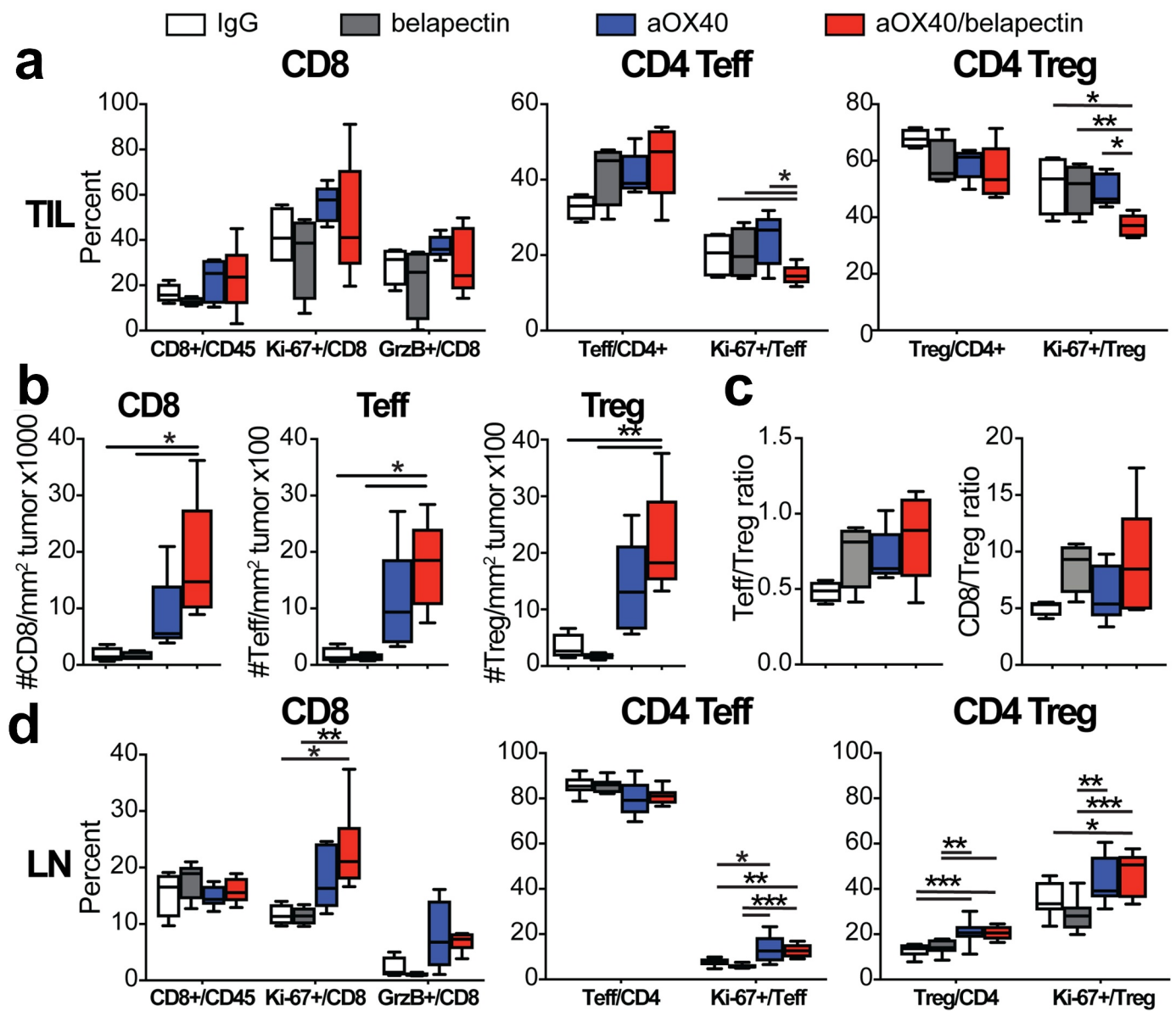
Figure 2. Combination aOX40/belapectin therapy increases CD8+ T cell density in the tumor. MCA-205 tumor-bearing mice were treated with IgG, aOX40 (days 10, 14), and/or belapectin (days 10, 12, 14, 16). Tumors were harvested on day 17 for analysis by flow cytometry, data presented as (A) percent of parent population and (B) density (cells/mm² tumor tissue). C) Ratio of Teff/Treg and CD8+/Treg densities. D) Flow cytometry data collected from lymph nodes collected the same day (day 17) as tumor harvest. Teff/Treg were identified by CD4+, FoxP3− or FoxP3+, respectively. Data from 2 independent experiments, n = 4/cohort; boxes depict median (line), 95% CI (box), and minimum/maximum values (whiskers); *P < .05, **P < .01, ***P < .001; 1-way ANOVA.

macrophages (TAMs; $CD11b^+Ly6C^{lo}Ly6G^{lo}F4/80^+$). TAMs can be further divided into MHC-II^{hi} or MHC-II^{lo} cells (Figure 3a). Each of these cell types can utilize varying mechanisms to suppress T cells including arginine depletion (arginase 1; Arg1), nitric oxide (NO) secretion (iNOS), and/or PD-1 engagement (PD-L1). For example, MHC-II^{lo} TAMs have been reported to exhibit increased Arg1 expression and are therefore categorized as M2-like alternatively polarized macrophages.[34] We noted that aOX40/belapectin therapy resulted in an influx of CD11b$^+$ cells into the tumor (Figure 3b) and therefore investigated phenotypic changes in M-MDSCs and/or other myeloid cell populations within the tumor. Anti-OX40/belapectin treatment reduced the frequency of M-MDSCs and MHC-II^{hi} TAMs and increased the percent of MHC-II^{lo} TAMs in

comparison to aOX40 monotherapy (Figure 3c). We also examined the potential suppressive function of these cell types based upon the expression of Arg1, iNOS, and PD-L1 (Figure 3d). Interestingly, M-MDSCs had increased iNOS and decreased PD-L1 expression following combination therapy compared to monotherapy controls (Figure 3e). Thus, tumors treated with aOX40/belapectin therapy had a reduced percentage of M-MDSCs, and the remaining cells exhibited a less suppressive phenotype.

Several significant differences were also observed in the phenotype of TAMs within the TME as both MHC-II^{hi} and MHC-II^{lo} subsets had increased expression of iNOS following combination therapy (Figure 3e). Interestingly, MHC-II^{lo} TAMs isolated from aOX40/belapectin -treated tumors also expressed significantly less Arg1, a commonly
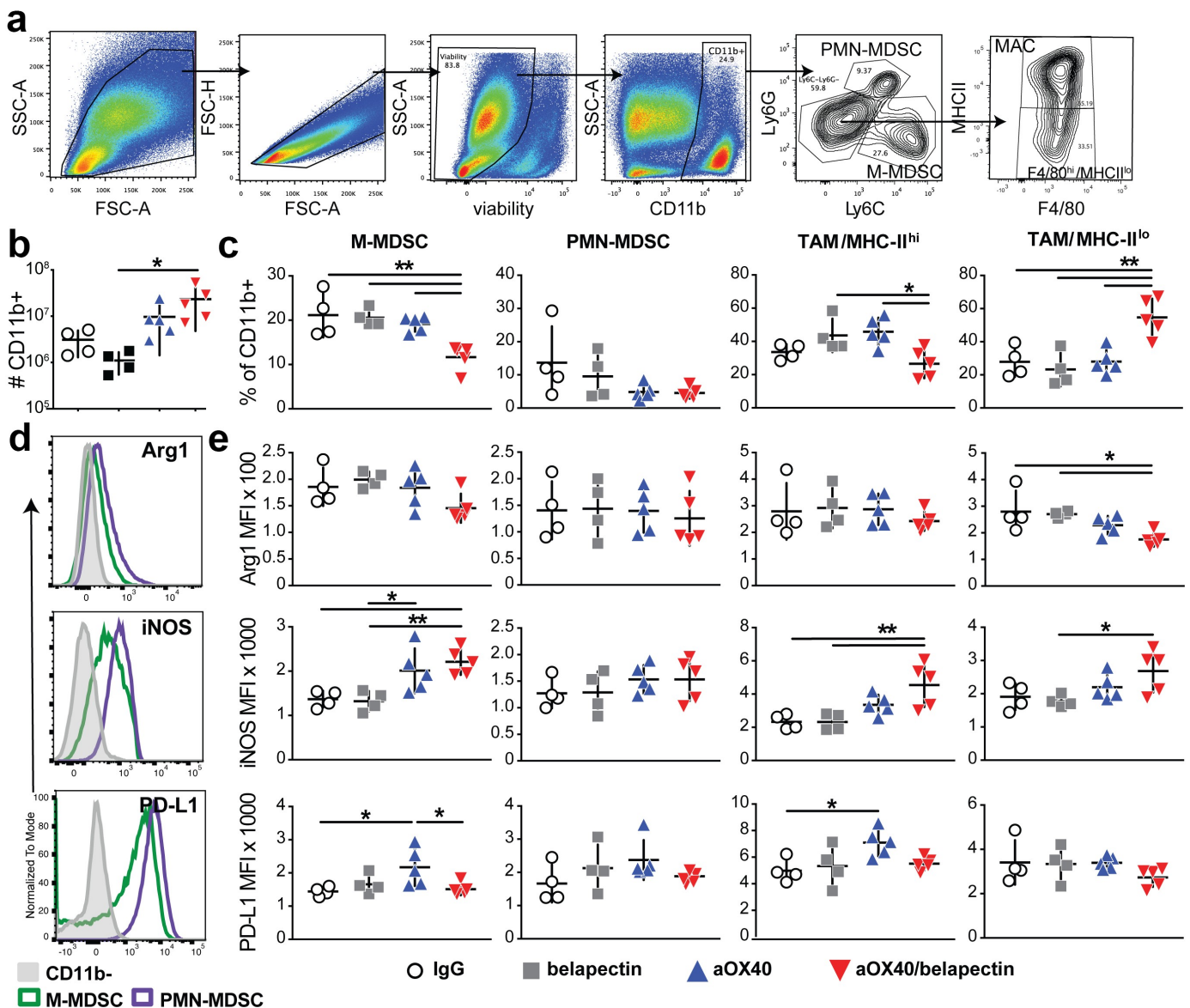
Figure 3. Combined aOX40/belapectin therapy decreases M-MDSCs within the tumor. MCA-205 tumor-bearing mice were treated as in Fig. 2. Tumors were harvested on day 17 for analysis by flow cytometry. A) Gating strategy to identify M-MDSC, PMN-MDSC, and TAMs. B-C) The total number of B) CD11b$^+$ cells and C) The frequency of M-MDSC, PNM-MDSC, and TAM/MHC-II^{hi}, TAM/MHC-II^{lo} of total CD11b$^+$ cells across treatment types. D) Representative histogram depicting Arg1, iNOS, and PD-L1 expression in M-MDSC (green, open) and PMN-MDSC (purple, open) compared to CD11b$^-$ cells (gray, filled). E) The MFI of Arg1, iNOS, and PD-L1 expression for each subset is shown. Data are representative of 1 of 2 independent experiments; mean ± SD; *P < .05, **P < .01; 1-way ANOVA.

reported M2 marker, in comparison to belapectin mono-therapy (Figure 3e). We confirmed these results by mIHC, where aOX40-treated tumors exhibited increased Arg1 co-staining with CD11b and F4/80, and conversely, combination therapy treated tumors exhibited increased iNOS co-staining with CD11b and F4/80 and a reduced ratio of Arg1:iNOS as compared to controls (Fig. S7). Together, these data indicate that aOX40/belapectin therapy modulates the composition of myeloid cell types within the tumor and significantly increases iNOS expression in M-MDSCs and TAMs, while reducing the extent of suppressive proteins such as Arg1 and PD-L1.

Combined aOX40/belapectin therapy reduces M-MDSC functional suppression within the TME

Anti-OX40/belapectin therapy induced an increased number of CD8$^+$ T cells when normalized to tumor size (Figure 2) and decreased percentage in M-MDSCs (Figure 3) in comparison to aOX40. We did not observe a difference in the density of M-MDSCs across treatments (Figure 4a), likely due to the increased total number of CD11b$^+$ cells in the tumor due to aOX40 (Figure 3b). However, the ratio of CD8$^+$ T cell: M-MDSCs, which, importantly, takes into account the number of immune cells compared to the size of the tumor, was increased 2.5-fold in tumors (Figure 4b). Thus, we found that
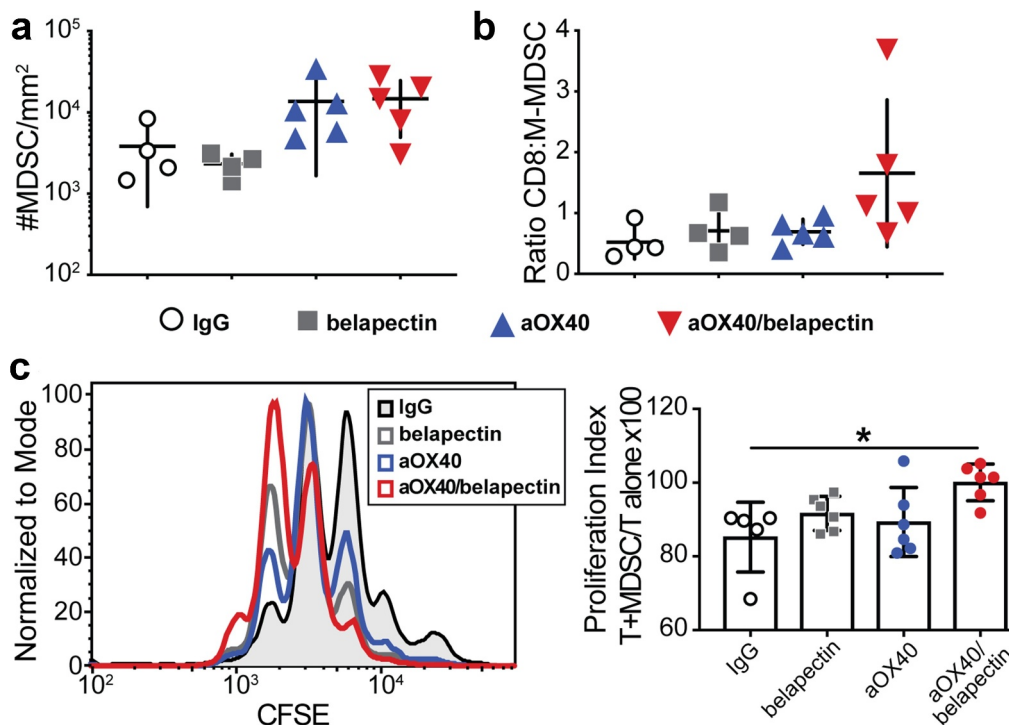
Figure 4. aOX40/belapectin therapy reduces the suppressive function of M-MDSC within the TME. MCA-205 tumor-bearing mice were treated as in Figure. 2 and tumors harvested on day 17. A) Density of M-MDSC per tumor across treatment groups. B) Ratio of CD8$^+$ T cells to M-MDSCs across treatment groups. Graphs depict the mean ± SD. C) M-MDSCs (CD11b$^+$Ly6C$^+$) were sorted from tumors and co-cultured (1:1) with CFSE-loaded naïve CD8$^+$ T cells isolated from spleens of wild-type mice and stimulated on aCD3-coated plates for 72 hrs. Representative histograms of CD8$^+$ T cell CFSE staining are shown. D) Graphs represent % Proliferation Index (PI) (Total # cell divisions/# cells divided) of CD8$^+$ T cells co-cultured with M-MDSCs divided by PI of T cells alone. Data depicts the mean ± SD of 2 independent experiments *P < .05 (1-way ANOVA).

combination therapy enhanced the ratio of CD8$^+$ T cells to two suppressive cell populations, CD4$^+$ Treg (Figure 2d) and M-MDSCs (Figure 4b) on a per tumor-size basis.

Combined aOX40/belapectin treatment was associated with increased CD8$^+$ T cell infiltration within the tumor (Figure 2) and with changes in the M-MDSC compartment suggesting reduced suppressive function (Figure 3). However, the presence of suppressive markers alone is not sufficient evidence of their suppressive activity.[35] Therefore, to test the hypothesis that the suppressor function of M-MDSCs is reduced due to aOX40/belapectin, we examined the ability of M-MDSCs isolated from aOX40/belapectin-treated tumors to functionally suppress CD8$^+$ T cell proliferation. CFSE-labeled naïve CD8$^+$ T cells were co-cultured with M-MDSCs isolated from tumors and the extent of CFSE dilution was determined after 72 hrs. Indeed, M-MDSCs isolated from aOX40/belapectin-treated mice exhibited reduced suppressive function as compared to M-MDSCs from either monotherapy-treated cohort (Figure 4c). To quantify this phenotype, we calculated the proliferation index (PI), which is based upon the number of total divisions of dividing cells. Comparison across treatment groups revealed a significantly increased PI within the aOX40/belapectin-treated cohort as compared to controls (Figure 4d). Together with the altered M-MDSC phenotype (Figure 3), these functional data demonstrate that aOX40/belapectin treatment alleviates M-MDSC-mediated T cell suppression.

Discussion

Although cancer immunotherapy can generate potent anti-tumor immunity against a variety of malignancies, several barriers limit its therapeutic efficacy in the majority of patients. For example, tumor-induced immunosuppression via tumor-intrinsic (e.g., increased expression of Gal-3, PD-L1, TGF-β, IL-10, anti-apoptotic molecules, etc.) or extrinsic (e.g., induction/recruitment of Treg, MDSCs, etc.) mechanisms often hinders the generation of curative responses. In the current study, we tested the hypothesis that inhibiting Gal-3 with belapectin would alleviate immune suppression within the TME, thereby boosting the efficacy of aOX40 immunotherapy. Indeed, using three different tumor models, we demonstrated that aOX40/belapectin therapy markedly increased tumor-free survival compared to controls (Figure 1(c-e)) in a CD8$^+$ T cell-dependent manner (figure 1f). Further studies revealed that combination therapy reduced the frequency and suppressive capacity of M-MDSCs within the TME (Figures 3C and Figures 4c, respectfully), which was associated with an increased density of CD8$^+$ T cells within the tumor (Figure 2b and Fig. S6). Taken together, these data demonstrate that aOX40/belapectin therapy alters the suppressive TME through a reduction in MDSC infiltration and suppressive function with a concomitant increase in IFN-γ-producing effector CD8$^+$ T cells (Fig. S5B).

Gal-3 is highly expressed in numerous tumor types including melanoma, head and neck squamous cell carcinoma (HNSCC), non-small cell lung cancer (NSCLC), breast,

cervical, and colorectal cancer among others.[16,20,36] Increased Gal-3 expression correlates with metastasis and is a negative prognostic indicator.[36-40] Gal-3 is also widely expressed and secreted by numerous cell types present within the TME including macrophages, fibroblasts, and activated T cells themselves and can exert immune suppression through increased M2 macrophage polarization and impaired T cell receptor signaling in the TME.[15,26,41,42] Thus, Gal-3 is under investigation as a therapeutic target to inhibit cancer,[43] and preclinical studies have demonstrated the ability of Gal-3 inhibitors to impact tumor growth and/or reduce metastasis. For example, GCS-100, a modified citrus pectin carbohydrate that binds Gal-3, limited metastasis of murine melanoma and rat prostate cancer cells, likely through inhibiting or interfering with cell-cell interactions driving metastasis through Gal-3.[24,44-47] Further, GCS-100 was shown to inhibit directly myeloma cell growth and induce apoptosis in vitro.[44] In our study, combination aOX40/belapectin therapy significantly reduced the incidence of spontaneous lung metastases in 4T1 tumor-bearing mice (Figure 1g). Although we did not observe any impact of belapectin monotherapy on tumor growth in vivo, our in vitro analyses revealed that belapectin monotherapy slightly increased apoptosis of 4T1 and MCA-205 tumor cells. We also detected the greatest benefit of aOX40/belapectin combination therapy in 4T1 and MCA-205 tumor-bearing mice. Tumor cells undergoing apoptosis are known to upregulate CD40L and release damage-associated molecular patterns (DAMPs) that can promote antigen presenting cell costimulation and activation, respectively.[48] Thus, our observation that aOX40/belapectin therapy boosted T cell priming in the LN (Figure 2d) may reflect increased tumor cell death, which subsequently may contribute to increased priming in vivo.

Recent work demonstrated that treatment with the small molecule Gal-3 inhibitor, GB1107, reduced the growth of human lung A549 adenocarcinoma xenografts and LLC1 tumors in vivo.[38] In addition, Gal-3 inhibition was associated with decreased expression of M2-polarized macrophages and increased CD8+ T cell infiltration in the tumor. Notably, the effects of GB1107 monotherapy were limited to early treatment (1 day post-tumor implant); when dosing was delayed until day 6 post-implantation, monotherapy had no impact on tumor burden, unless treatment was combined with PD-1 blockade. In the current study, we observed a similar lack of monotherapy efficacy as belapectin treatment alone had little to no impact on tumor growth and metastasis (Figure 1). However, in combination with aOX40 therapy, we observed a significant reduction in tumor burden and concomitant increase in survival in mice across multiple tumor models including TRAMP-C1, 4T1, and MCA-205 (Figure 1). Further analysis revealed that aOX40/belapectin therapy altered the TME through a reduction in the frequency and suppressive function of M-MDSCs (Figure 4c) along with a subsequent increase in cytotoxic CD8+ T cell infiltration (Figure 2b and Fig. S6). Recent work also showed that Gal-3 blockade restored IFN-γ production by CD8+ T cells in vitro,[24,49] supporting the hypothesis that Gal-3 functionally impairs TCR signaling.[41,42] Whether aOX40/belapectin therapy alters TCR signaling is currently under investigation, but we believe this is unlikely to be the major mechanism of action because related metrics of CD8+ T cell function, including granzyme B expression and IFN-γ production, are relatively similar between the aOX40 monotherapy and aOX40/belapectin cohorts (Figure 2a, Figure 2d and Fig. S5B). In contrast, we observed a robust decrease in total M-MDSCs (Figure 3c) and their expression of Arg1 and PD-L1, in conjunction with increased iNOS (Figure 3c). Along with the significant increase in MHC-II^hi TAMs (Figure 3c), we believe this reflects repolarization of the TME to favor tumor rejection. One potential mechanism that may facilitate TAM reprogramming is through altered cytokine distribution within the TME. For example, recent work suggested that Gal-3 hinders the ability of IFN-γ to diffuse through the tumor matrix, thereby minimizing CXCL9 secretion by tumors cells in response. The overall effect led to the reduction of CD8+ T cells trafficking to the tumor.[25]

The presence of MDSCs in the tumor predicts reduced overall survival and poor disease-free survival across multiple tumor types.[50] MDSCs encompass a heterogeneous population of immature myeloid cells that suppress both innate and adaptive immunity through inhibiting T cell proliferation and decreasing cytokine secretion. While MDSCs can be identified phenotypically, due to their heterogeneous nature the 'gold standard' to identify MDSCs is to demonstrate their suppressive capabilities.[35] We found that aOX40/belapectin combination therapy not only reduced the suppressive capacity of MDSCs, but also reduced the overall percent of MDSCs suggesting that combination therapy prevents their generation and/or migration. Gal-3 has been reported as a chemoattractant for myeloid cells,[28,51] thus inhibiting Gal-3 with belapectin may prevent myeloid cell migration to the tumor. Macrophages also impede CD8+ T cells from entering the tumor,[52] so a reduction in myeloid cells due to Gal-3 inhibition could result in increased CD8+ T cell infiltration, which we also observed as a result of combination therapy. This could start a feed-forward loop, whereby the cytokine milieu, now dominated by activated CD8+ T cells and Th1 cytokines in the tumor, determines the fate of myeloid cells,[53] which take on a more M1-like, anti-tumor phenotype.

In summary, our data highlights the therapeutic potential of Gal-3 inhibition in conjunction with aOX40 immunotherapy to inhibit metastasis and reprogram the TME to favor M1 macrophage polarization and the generation of potent effector CD8+ T cells responses. Notably, belapectin appeared safe and well-tolerated in previous clinical studies and is currently being evaluated in a phase I trial in combination with checkpoint blockade at our institution (NCT02575404). Thus, we believe that these results support the evaluation of aOX40/belapectin combination therapy in future clinical trials.

ORCID

Annah S. Rolig http://orcid.org/0000-0001-7080-4352
William L. Redmond http://orcid.org/0000-0002-2572-1731

Declarations

No potential conflicts of interest were disclosed.

Ethics approval and consent to participate

No human subjects were part of this research. Animal studies were performed in accordance with the National Institutes of Health Guide for the Care and Use of Laboratory Animals and with the approval of the Earle A. Chiles Research Institute Institutional Animal Care and Use Committee (Animal Welfare Assurance No. A3913–01).

Availability of data and material

The datasets used and/or analyzed during the current study are available from the corresponding author upon reasonable request. Belapectin is available from Galectin Therapeutics upon reasonable request.

Competing interests

William Redmond has received research funding from Galectin Therapeutics, Bristol-Myers Squibb, AstraZeneca, Merck, Nektar Therapeutics, GlaxoSmithKline, Aeglea BioTherapeutics, Shimadzu, Inhibrx, Veana Therapeutics, OncoSec, Calibr, and MiNA Therapeutics, is on the advisory board of Vesselon, and receives licensing fees from Galectin Therapeutics. Peter Traber is a stockholder of Galectin Therapeutics and employee and stockholder of Selecta Biosciences. Harold Shlevin is an employee of Galectin Therapeutics. All other authors declare they have no competing interests.

References

1. Sharma P, Allison JP. The future of immune checkpoint therapy. Science. 2015;348(6230):56–61. doi:10.1126/science.aaa8172.
2. Redmond WL, Gough MJ, Weinberg AD. Ligation of the OX40 co-stimulatory receptor reverses self-Ag and tumor-induced CD8 T-cell anergy in vivo. Eur J Immunol. 2009;39(8):2184–2194. doi:10.1002/eji.200939348.
3. Gough MJ, Ruby CE, Redmond WL, Dhungel B, Brown A, Weinberg AD. OX40 agonist therapy enhances CD8 infiltration and decreases immune suppression in the tumor. Cancer Res. 2008;68(13):5206–5215. doi:10.1158/0008-5472.CAN-07-6484.
4. Redmond WL, Gough MJ, Charbonneau B, Ratliff TL, Weinberg AD. Defects in the acquisition of CD8 T cell effector function after priming with tumor or soluble antigen can be overcome by the addition of an OX40 agonist. J Immunol. 2007;179 (11):7244–7253. doi:10.4049/jimmunol.179.11.7244.
5. Ruby CE, Redmond WL, Haley D, Weinberg A. Anti-OX40 stimulation in vivo enhances CD8+ memory T cell survival and significantly increases recall responses. Eur J Immunol. 2007;37 (1):157–166. doi:10.1002/eji.200636428.
6. Esfahani K, Roudaia L, Buhlaiga N, Del Rincon SV, Papneja N, Miller WH. A review of cancer immunotherapy: from the past, to the present, to the future. Curr Oncol. 2020;27(Suppl2):S87–S97. doi:10.3747/co.27.5223. [published Online First: 04/01]
7. Redmond WL, Ruby CE, Weinberg AD. The role of OX40-mediated co-stimulation in T-cell activation and survival. Crit Rev Immunol. 2009;29(3):187–201. doi:10.1615/CritRevImmunol.v29.i3.10.
8. Redmond WL, Weinberg AD. Targeting OX40 and OX40L for the treatment of autoimmunity and cancer. Crit Rev Immunol. 2007;27(5):415–436. doi:10.1615/CritRevImmunol.v27.i5.20.

9. Rogers PR, Song J, Gramaglia I, Killeen N, Croft M. OX40 promotes Bcl-xL and Bcl-2 expression and is essential for long-term survival of CD4 T cells. Immunity. 2001;15(3):445–455. doi:10.1016/S1074-7613(01)00191-1.
10. Linch SN, Kasiewicz MJ, McNamara MJ, Hilgart-Martiszus IF, Farhad M, Redmond WL. Combination OX40 agonism/CTLA-4 blockade with HER2 vaccination reverses T-cell anergy and promotes survival in tumor-bearing mice. Proc Natl Acad Sci U S A. 2016;113(3):E319–27. doi:10.1073/pnas.1510518113.
11. Murata S, Ladle BH, Kim PS, Lutz ER, Wolpoe ME, Ivie SE, Smith HM, Armstrong TD, Emens LA, Jaffee EM, et al. OX40 costimulation synergizes with GM-CSF whole-cell vaccination to overcome established CD8+ T cell tolerance to an endogenous tumor antigen. J Immunol. 2006;176(2):974–983. doi:10.4049/jimmunol.176.2.974.
12. Curti BD, Kovacsovics-Bankowski M, Morris N, Walker E, Chisholm L, Floyd K, Walker J, Gonzalez I, Meeuwsen T, Fox BA, et al. OX40 is a potent immune-stimulating target in late-stage cancer patients. Cancer Res. 2013;73(24):7189–7198. doi:10.1158/0008-5472.CAN-12-4174.
13. Redmond WL, Linch SN, Kasiewicz MJ. Combined targeting of costimulatory (OX40) and coinhibitory (CTLA-4) pathways elicits potent effector T cells capable of driving robust antitumor immunity. Cancer Immunol Res. 2014;2(2):142–153. doi:10.1158/2326-6066.CIR-13-0031-T.
14. Linch SN, Redmond WL. Combined OX40 ligation plus CTLA-4 blockade: more than the sum of its parts. Oncoimmunology. 2014;3:e28245. doi:10.4161/onci.28245.
15. Dumic J, Dabelic S, Flogel M. Galectin-3: an open-ended story. Biochim Biophys Acta. 2006;1760(4):616–635. doi:10.1016/j.bbagen.2005.12.020. [published Online First: 2006/02/16]
16. Farhad M, Rolig AS, Redmond WL. The role of Galectin-3 in modulating tumor growth and immunosuppression within the tumor microenvironment. Oncoimmunology. 2018;7(6):e1434467. doi:10.1080/2162402X.2018.1434467. [published Online First: 2018/06/07]
17. Cerliani JP, Blidner AG, Toscano MA, Croci DO, Rabinovich GA. Translating the 'sugar code' into immune and vascular signaling programs. Trends Biochem Sci. 2017;42(4):255–273. doi:10.1016/j.tibs.2016.11.003.
18. Ruvolo PP. Galectin 3 as a guardian of the tumor microenvironment. Biochimi Et Biophys Acta (BBA) - Mol Cell Res. 2016;1863(3):427–437. doi:10.1016/j.bbamcr.2015.08.008.
19. Jiang SS, Weng DS, Wang QJ, Pan K, Zhang YJ, Li YQ, Li JJ, Zhao JJ, He J, Lv L, Pan QZ. Galectin-3 is associated with a poor prognosis in primary hepatocellular carcinoma. J Transl Med. 2014;12:273. [published Online First: 2014/09/28]. doi:10.1186/s12967-014-0273-3.
20. Wang Y, Liu S, Tian Y, Wang Y, Zhang Q, Zhou X, Meng X, Song N. Prognostic role of galectin-3 expression in patients with solid tumors: a meta-analysis of 36 eligible studies. Cancer Cell Int. 2018;18(1):172. doi:10.1186/s12935-018-0668-y.
21. Capalbo C, Scafetta G, Filetti M, Marchetti P, Bartolazzi A. Predictive biomarkers for checkpoint inhibitor-based immunotherapy: the Galectin-3 signature in NSCLCs. Int J Mol Sci. 2019;20(7). [published Online First: 2019/04/03]. doi:10.3390/ijms20071607.
22. Thijssen VL, Heusschen R, Caers J, Griffioen AW. Galectin expression in cancer diagnosis and prognosis: a systematic review. Biochimi Et Biophys Acta (BBA) - Rev Cancer. 2015;1855 (2):235–247. doi:10.1016/j.bbcan.2015.03.003.
23. Henderson NC, Sethi T. The regulation of inflammation by galectin-3. Immunol Rev. 2009;230(1):160–171. doi:10.1111/j.1600-065X.2009.00794.x.
24. Demotte N, Wieers G, Van Der Smissen P, Moser M, Schmidt C, Thielemans K, Squifflet J-L, Weynand B, Carrasco J, Lurquin C, et al. A galectin-3 ligand corrects the impaired function of human CD4 and CD8 tumor-infiltrating lymphocytes and favors tumor rejection in mice. Cancer Res. 2010;70(19):7476–7488. [published Online First: 2010/08/20]. doi:10.1158/0008-5472.CAN-10-0761.
25. Gordon-Alonso M, Hirsch T, Wildmann C, van der Bruggen P. Galectin-3 captures interferon-gamma in the tumor matrix reducing chemokine gradient production and T-cell tumor infiltration. Nat

Commun. 2017;8(1):793. [published Online First: 2017/10/08]. doi:10.1038/s41467-017-00925-6.

26. MacKinnon AC, Farnworth SL, Hodkinson PS, et al. Regulation of alternative macrophage activation by galectin-3. J Immunol. 2008;180(4):2650–2658. [pii] [published Online First: 2008/02/06]. doi:10.4049/jimmunol.180.4.2650

27. Wang T, Chu Z, Lin H, Jiang J, Zhou X, Liang X. Galectin-3 contributes to cisplatin-induced myeloid derived suppressor cells (MDSCs) recruitment in Lewis lung cancer-bearing mice. Mol Biol Rep. 2014;41(6):4069–4076. doi:10.1007/s11033-014-3276-5.

28. Sano H, Hsu DK, Yu L, Apgar JR, Kuwabara I, Yamanaka T, Hirashima M, Liu FT. Human galectin-3 is a novel chemoattractant for monocytes and macrophages. J Immunol. 2000;165 (4):2156–2164. doi:10.4049/jimmunol.165.4.2156.

29. Traber PG, Zomer E. Therapy of experimental NASH and fibrosis with galectin inhibitors. PloS One. 2013;8(12):e83481. doi:10.1371/journal.pone.0083481.

30. Chalasani N, Abdelmalek MF, Garcia-Tsao G, Vuppalanchi R, Alkhouri N, Rinella M, Noureddin M, Pyko M, Shiffman M, Sanyal A, et al. Effects of belapectin, an inhibitor of galectin-3, in patients with nonalcoholic steatohepatitis with cirrhosis and portal hypertension. Gastroenterology. 2020;158(5):1334–45e5. [published Online First: 2019/12/10]. doi:10.1053/j.gastro.2019.11.296.

31. Pulaski BA, Mouse O-RS. 4T1 breast tumor model. Curr Protoc Immunol. Chapter 20:Unit20 2. doi: 10.1002/0471142735. im2002s39 [published Online First: 2008/04/25]. 2001. doi:.

32. Crittenden MR, Savage T, Cottam B, Bahjat KS, Redmond WL, Bambina S, Kasiewicz M, Newell P, Jackson AM, Gough MJ, et al. The peripheral myeloid expansion driven by murine cancer progression is reversed by radiation therapy of the tumor. PloS One. 2013;8(7):e69527. doi:10.1371/journal.pone.0069527.

33. Giordano M, Croci DO, Rabinovich GA. Galectins in hematological malignancies. Curr Opin Hematol. 2013;20(4):327–335. doi:10.1097/MOH.0b013e328362370f.

34. Laoui D, Van Overmeire E, Di Conza G, Aldeni C, Keirsse J, Morias Y, Movahedi K, Houbracken I, Schouppe E, Elkrim Y, et al. Tumor hypoxia does not drive differentiation of tumor-associated macrophages but rather fine-tunes the M2-like macrophage population. Cancer Res. 2014;74(1):24. doi:10.1158/0008-5472.CAN-13-1196.

35. Bronte V, Brandau S, Chen SH, Colombo MP, Frey AB, Greten TF, Mandruzzato S, Murray PJ, Ochoa A, Ostrand-Rosenberg S, Rodriguez PC. Recommendations for myeloid-derived suppressor cell nomenclature and characterization standards. Nat Commun. 2014;12(1):12150. [published Online First: 2016/07/07]. doi:10.1186/s12967-014-0273-3.

36. Dube-Delarosbil C, St-Pierre Y. The emerging role of galectins in high-fatality cancers. Cell Mol Life Sci. 2018;75(7):1215–1226. doi:10.1007/s00018-017-2708-5. [published Online First: 2017/11/10]

37. Mathieu A, Saal I, Vuckovic A, Ransy V, Vereerstraten P, Kaltner H, Gabius HJ, Kiss R, Decaestecker C, Salmon I, et al. Nuclear galectin-3 expression is an independent predictive factor of recurrence for adenocarcinoma and squamous cell carcinoma of the lung. Mod Pathol. 2005;18(9):1264–1271. [published Online First: 2005/04/16]. doi:10.1038/modpathol.3800416.

38. Vuong L, Kouverianou E, Rooney CM, McHugh BJ, Howie SE, Gregory CD, Forbes SJ, Henderson NC, Zetterberg FR, Nilsson UJ, et al. An orally active galectin-3 antagonist inhibits lung adenocarcinoma growth and augments response to PD-L1 blockade. Cancer Res. 2014;41(6):4069–4076. [published Online First: 2019/01/25]. doi:10.1007/s11033-014-3276-5.

39. Matsuda Y, Yamagiwa Y, Fukushima K, Ueno Y, Shimosegawa T. Expression of galectin-3 involved in prognosis of patients with hepatocellular carcinoma. Hepatol Res. 2008;38(11):1098–1111.

40. Honjo Y, Inohara H, Akahani S, Yoshii T, Takenaka Y, Yoshida J, Hattori K, Tomiyama Y, Raz A, Kubo T, et al. Expression of cytoplasmic galectin-3 as a prognostic marker in tongue carcinoma. Clin Cancer Res : An off J Am Assoc Cancer Res. 2000;6(12):4635–4640. [published Online First: 2001/01/13].

41. Chen H-Y, Fermin A, Vardhana S, Weng I-C, Lo KFR, Chang E-Y, Maverakis E, Yang R-Y, Hsu DK, Dustin ML, et al. Galectin-3 negatively regulates TCR-mediated CD4+ T-cell activation at the immunological synapse. Proc Natl Acad Sci U S A. 2009;106 (34):14496–14501. [published Online First: 2009/08/27]. doi:10.1073/pnas.0903497106.

42. Hsu DK, Chen H-Y, Liu F-T. Galectin-3 regulates T-cell functions. Immunol Rev. 2009;230(1):114–127. doi:10.1111/j.1600-065X.2009.00798.x. [published Online First: 2009/07/15]

43. Blanchard H, Yu X, Collins PM, Bum-Erdene K. Galectin-3 inhibitors: a patent review (2008–present). Expert Opin Ther Pat. 2014;24(10):1053–1065. doi:10.1517/13543776.2014.947961. [published Online First: 2014/08/12]

44. Streetly MJ, Maharaj L, Joel S, Schey SA, Gribben JG, Cotter FE. GCS-100, a novel galectin-3 antagonist, modulates MCL-1, NOXA, and cell cycle to induce myeloma cell death. Blood. 2010;115 (19):3939–3948. doi:10.1182/blood-2009-10-251660. [published Online First: 2010/03/02]

45. Pienta KJ, Nailk H, Akhtar A, Yamazaki K, Replogle TS, Lehr J, Donat TL, Tait L, Hogan V, Raz A, et al. Inhibition of spontaneous metastasis in a rat prostate cancer model by oral administration of modified citrus pectin. J Natl Cancer Inst. 1995;87(5):348–353. doi:10.1093/jnci/87.5.348.

46. Inohara H, Raz A. Effects of natural complex carbohydrate (citrus pectin) on murine melanoma cell properties related to galectin-3 functions. Glycoconj J. 1994 [published Online First: 1994/12/01];11(6):527–532. doi:10.1007/BF00731303.

47. Platt D, Raz A. Modulation of the lung colonization of B16-F1 melanoma cells by citrus pectin. J Natl Cancer Inst. 1992;84 (6):438–442. doi:10.1093/jnci/84.6.438.

48. Bonaventura P, Shekarian T, Alcazer V, Valladeau-Guilemond J, Valsesia-Wittmann S, Amigorena S, Caux C, Depil S. Cold tumors: a therapeutic challenge for immunotherapy. Front Immunol. 2019;10:168. doi:10.3389/fimmu.2019.00168.

49. Demotte N, Stroobant V, Courtoy PJ, Van Der Smissen P, Colau D, Luescher IF, Hivroz C, Nicaise J, Squifflet J-L, Mourad M, et al. Restoring the association of the T cell receptor with CD8 reverses anergy in human tumor-infiltrating lymphocytes. Immunity. 2008;28(3):414–424. [published Online First: 2008/03/18]. doi:10.1016/j.immuni.2008.01.011.

50. Ai L, Mu S, Wang Y, Wang H, Cai L, Li W, Hu Y. Prognostic role of myeloid-derived suppressor cells in cancers: a systematic review and meta-analysis. BMC Cancer. 2018;18(1):1220. doi:10.1186/s12885-018-5086-y. [published Online First: 2018/12/07]

51. Jia W, Kidoya H, Yamakawa D, Naito H, Takakura N. Galectin-3 accelerates M2 macrophage infiltration and angiogenesis in tumors. Am J Pathol. 2013;182(5):1821–1831. doi:10.1016/j.ajpath.2013.01.017. [published Online First: 2013/03/19]

52. Peranzoni E, Lemoine J, Vimeux L, Feuillet V, Barrin S, Kantari-Mimoun C, Bercovici N, Guérin M, Biton J, Ouakrim H, et al. Macrophages impede CD8 T cells from reaching tumor cells and limit the efficacy of anti–PD-1 treatment. Proc Natl Acad Sci U S A. 2018;115(17):E4041–E50. [published Online First: 2018/04/11]. doi:10.1073/pnas.1720948115.

53. Umansky V, Blattner C, Gebhardt C, Utikal J. The role of Myeloid-Derived Suppressor Cells (MDSC) in cancer progression. Vaccines (Basel). 2016;4(4). doi:10.3390/vaccines4040036. [published Online First: 2016/11/10]

doi:10.1111/j.1872-034X.2008.00387.x. [published Online First: 2008/08/08]